Effects of interfacial transport on the equilibrium fluctuations in fluid layers

Dina Gutkowicz-Krusin
Corporate Research—Science Laboratories, Exxon Research and Engineering Company, Linden, New Jersey 07036

Itamar Procaccia
Department of Chemical Physics, Weizmann Institute of Science, Rehovot 76100, Israel
(Received 27 September 1982)

Complete hydrodynamic theory of the dynamics of equilibrium fluctuations in one-component fluid layers confined by rigid solid boundaries is presented. The dynamic structure factor for such a fluid layer is shown to have both diagonal and off-diagonal elements which depend on the layer height L and on the transport of energy and tangential momentum across the fluid-solid interfaces. The effects of interfacial energy transport have been analyzed in the limits of maximum or vanishing tangential momentum transport ("stick" or "slip" boundary conditions on the velocity field). In the presence of interfacial transport, two new propagating modes have been found for each distinct interface. In the limit of maximum energy and/or tangential momentum transport, the new modes differ from the bulk sound modes only by an increased attenuation coefficient. Additional dissipation is in part due to shear created by the boundaries, and in part, since the sound is not isothermal, to heat conduction between the fluid and solid. In the dynamic structure factor, the new modes appear as additional peaks in the vicinity of the Brillouin peaks of the unbounded fluid; for wave vectors typical of light scattering experiments these peaks are found to be significant for $L \sim 100\ \mu$m. Since the positions and line shapes of these peaks are very sensitive to interfacial transport, their study may provide a useful experimental probe of transport across the fluid-solid interfaces.

I. INTRODUCTION

The dynamic properties of fluids confined by solid boundaries may be significantly affected by the transport of mass, momentum, and energy across the fluid-solid interfaces.[1] In the hydrodynamic regime, such interfacial transport is traditionally modeled by empirical boundary conditions on the hydrodynamic variables such as temperature and velocity. For example, for rigid interfaces, the absence of interfacial mass transport leads to a boundary condition of continuity of the component of velocity normal to interfaces. If there is no tangential momentum transport, the fluid "slips" along the interface and the tangential components of stress must vanish. If, however, the tangential momentum transport is maximum, the fluid "sticks" to the interface across which the tangential components of velocity must be continuous. In addition, it is usually assumed that the heat and entropy fluxes are continuous across the interfaces, resulting in the boundary conditions of continuity of temperature and heat flux.

These boundary conditions are well established experimentally; however, their experimental determination is typically based on time-independent macroscopic flow properties.[2,3] There has been no sensitive experimental study of interfacial transport over a wide frequency range. In addition, there exist no complete theories, either molecular or phenomenological (based on ideas of nonequilibrium thermodynamics), of the very complex problem of transport across the fluid-solid interfaces. In a recent paper,[1] we presented some results on effects of interfacial transport on the dynamics of the equilibrium fluid fluctuations and suggested that the experiments which determine the dynamics of fluid fluctuations (light and neutron scattering, sound attenuation and dispersion) may prove to be useful probes of interfacial transport over a wide frequency range.

In this paper, we present the complete hydrodynamic theory of fluctuations in one-component fluid layers confined by rigid solid walls. Since in equilibrium the fluid fluctuations obey the linearized hydrodynamic equations,[3] it is necessary to solve them subject to the appropriate boundary conditions at the solid walls. For simplicity, we assume the fluid layer to be of infinite extent in the xy plane and of height L. Thus, interfacial transport affects the fluctuations only through the boundary conditions at $z=\pm L/2$. Since we are interested in time-dependent autocorrelation functions of hydrodynamic variables, we have an initial boundary value problem which can be solved most easily by introducing the Laplace transform in time (this leads to dependence on the variable $s=i\omega$) and the Fourier transform in the xy plane (this leads to dependence on the component of wave vector parallel to the interfaces $k_{\parallel}$). Thus, the problem is reduced to a one-dimensional one, which depends only on variable z. This problem can be solved exactly for any boundary conditions; the exact solutions for hydrodynamic variables are given in Sec. II.

The quantity of experimental interest is the dynamic structure factor, which is the Fourier transform of the time-dependent density autocorrelation function. The exact expression for the dynamic structure factor for any boundary conditions is given in Sec. III. It is found that, in contrast to the spectrum of fluctuations in unbounded fluid, the dynamic structure factor in a fluid layer has nonvanishing off-diagonal elements. These correlations between modes with different values of $k_{\perp}$ are due to the boundary conditions: in general, the Fourier modes are not the normal modes of the system.

The interfacial transport and boundary conditions are discussed in Sec. IV, while Secs. V and VI contain the results for the dynamic structure factor in the cases of stick and slip boundary conditions on the velocity field. It is shown that for most empirical boundary conditions (nonvanishing interfacial transport of either energy or tangential momentum) there exist in fluid layers two new modes for each distinct interface. These modes propagate parallel to the interfaces and their dispersion relation depends only on $k_{\parallel}$. In the extreme limits of infinite or vanishing thermal conductivity of the solid boundaries, these modes differ from the bulk sound modes only by increased attenuation coefficients. The physical interpretation of this additional dissipation is simple: The walls may (for stick boundary conditions on the velocity field) create additional shear in the fluid and may (if they are not insulating) act as a heat sink. Therefore, the additional term in the attenuation coefficient depends on the shear viscosity of the fluid and the thermal conductivity of both the fluid and solid walls. Hence, it is not surprising that in the case of slip boundary conditions and thermally insulating walls, these new interfacial modes disappear. For intermediate values of the thermal conductivity of the walls, the effective speed of the interfacial modes may have a nonanalytic dependence on $k_{\parallel}$.

In the dynamic structure factor, the interfacial modes appear as additional peaks in the vicinity of the Brillouin peaks of the infinite fluid. Their amplitudes are discussed in detail in Secs. V and VI. For wave vectors typical of light scattering experiments, they are found to become significant only for small values of L, on the order of ~ 100 μm. Nevertheless, since the positions and line shapes of these peaks are very sensitive to interfacial transport, their study may provide a useful experimental probe of transport across the fluid-solid interfaces. The results are summarized in Sec. VII.

II. DYNAMICS OF FLUCTUATIONS IN A FLUID LAYER

Consider a fluid layer of infinite extent in the xy plane and of height L in the z direction. The dynamics of a one-component fluid is given by the time dependence of the velocity field $\vec{u}$ and two independent thermodynamic variables, which can be conveniently chosen as the mass density ρ and temperature T.[3,4] Using the assumption of local thermal equilibrium, the other thermodynamic variables, such as pressure p or entropy density s, are determined uniquely in terms of ρ and T. In equilibrium $\langle\vec{u}\rangle=0$, $\langle\rho\rangle=\rho_0$, and $\langle T\rangle=T_0$, where the brackets denote equilibrium average. The dynamics of equilibrium fluctuations $\vec{u}$, $\delta\rho$, and δT in the fluid can be found from the solutions of the linearized hydrodynamic equations[3,4]

$$\frac{\partial\delta\rho}{\partial t}+\rho_0(\vec{\nabla}\cdot\vec{u})=0\ , \tag{2.1}$$

$$\frac{\partial\vec{u}}{\partial t}+\frac{c^2}{\gamma\rho_0}(\vec{\nabla}\delta\rho+\alpha\rho_0\vec{\nabla}\delta T)-\nu\nabla^2\vec{u}-(\Gamma_v-\nu)\vec{\nabla}(\vec{\nabla}\cdot\vec{u})=0\ , \tag{2.2}$$

$$\frac{\partial\delta T}{\partial t}+\frac{(\gamma-1)}{\alpha}(\vec{\nabla}\cdot\vec{u})-\gamma\kappa\nabla^2\delta T=0\ , \tag{2.3}$$

where c is the adiabatic speed of sound, $\gamma=C_p/C_v$, α is the thermal expansion coefficient, κ is the thermal diffusivity, ν and ζ are the shear and bulk kinematic viscosities, and $\Gamma_v\equiv\zeta+\frac{4}{3}\nu$ is the longitudinal viscosity.

The equilibrium dynamic correlation functions of fluctuations $\langle\delta A_i(\vec{r},t)\delta A_j(\vec{r}\,',0)\rangle$, where δA_i is any of the variables $\delta\rho$, δT, and $\vec{u}$, can be obtained from Eqs. (2.1)–(2.3) in either of two ways. In one approach, the fluctuating stress tensor and heat flux, whose correlations are assumed to be known, are added to Eqs. (2.2) and (2.3), respectively.[3] In the other approach, the set of Eqs. (2.1)–(2.3) is considered an initial value problem, and the dynamic correlation functions are found in terms of the static (equal time) correlation functions $\langle\delta A_i(\vec{r},0)\delta A_j(\vec{r}\,',0)\rangle$ (see Ref. 4). In this paper, the second approach is adopted since the correlation functions of the fluctuating stress tensor and heat flux are not easy to determine in the presence of fluid-solid interfaces, while the static correlation functions in such systems can be studied, at least in principle, both experimentally (by light or neutron scattering) and theoretically (by molecular dynamics).

The initial value problem in a fluid of infinite extent in the xy plane can be solved most easily by taking the Fourier transform of Eqs. (2.1)–(2.3) in the xy plane, and taking the Laplace transform of these equations in time. Then a fluctuating hydrodynamic variable δA_i is transformed to

$$\widetilde{A}_i(k_{\parallel},z;s)=\frac{1}{(2\pi)^2}\int_0^{\infty}dt\int_{-\infty}^{\infty}dx\int_{-\infty}^{\infty}dy\,\exp[-st-i(k_xx+k_yy)]\delta A_i(\vec{r},t)\;, \tag{2.4}$$

where

$$k_{\parallel}^2\equiv k_x^2+k_y^2\;.$$

This reduces Eqs. (2.1)–(2.3) to a system of ordinary differential equations in variable z:

$$s\widetilde{\rho}+\rho_0\left[\frac{d\widetilde{u}_z}{dz}+\widetilde{\phi}\right]=\delta\rho(k_{\parallel},z;0)\equiv\delta\rho(z)\;, \tag{2.5}$$

$$s\widetilde{T}-\gamma\kappa\left[\frac{d^2}{dz^2}-k_{\parallel}^2\right]\widetilde{T}+\frac{(\gamma-1)}{\alpha}\left[\frac{d\widetilde{u}_z}{dz}+\widetilde{\phi}\right]=\delta T(k_{\parallel},z;0)\equiv\delta T(z)\;, \tag{2.6}$$

$$s\widetilde{u}_z+\frac{c^2}{\gamma\rho_0}\left[\frac{d\widetilde{\rho}}{dz}+\alpha\rho_0\frac{d\widetilde{T}}{dz}\right]-\Gamma_v\frac{d^2\widetilde{u}_z}{dz^2}+\nu k_{\parallel}^2\widetilde{u}_z-(\Gamma_v-\nu)\frac{d\widetilde{\phi}}{dz}=u_z(k_{\parallel},z;0)\equiv u_z(z)\;, \tag{2.7}$$

$$s\widetilde{\phi}-\frac{c^2k_{\parallel}^2}{\gamma\rho_0}(\widetilde{\rho}+\alpha\rho_0\widetilde{T})-\nu\frac{d^2\widetilde{\phi}}{dz^2}+\Gamma_vk_{\parallel}^2\widetilde{\phi}+(\Gamma_v-\nu)k_{\parallel}^2\frac{d\widetilde{u}_z}{dz}=\phi(k_{\parallel},z;0)\equiv\phi(z)\;, \tag{2.8}$$

where

$$\phi\equiv\frac{\partial u_x}{\partial x}+\frac{\partial u_y}{\partial y}\;. \tag{2.9}$$

Equations (2.5)–(2.8) are to be solved subject to the appropriate boundary conditions on the variables $\widetilde{T}$, $\widetilde{u}_z$, and $\widetilde{\phi}$ at $z=\pm\frac{1}{2}L$. These boundary conditions and their influence on the dynamics of equilibrium fluctuations in fluid layers are discussed in detail in the following sections. Here, a general solution of Eqs. (2.5)–(2.8), valid for any boundary conditions, is constructed.

Using Eq. (2.5), $\widetilde{\rho}$ can be eliminated from Eqs. (2.6)–(2.8). Let $\vec{F}(z)$ be a vector such that

$$\vec{F}^T=\left[\widetilde{T},\frac{d\widetilde{T}}{dz},\widetilde{u}_z,\frac{d\widetilde{u}_z}{dz},\widetilde{\phi},\frac{d\widetilde{\phi}}{dz}\right]\;. \tag{2.10}$$

Then, it is straightforward to show that Eqs. (2.6)–(2.8) are equivalent to

$$\frac{d\vec{F}}{dz}=\underline{M}\vec{F}+\vec{f}\;, \tag{2.11}$$

where

$$\underline{M}=\begin{bmatrix} 0 & 1 & 0 & 0 & 0 & 0\\ \dfrac{s+\gamma\kappa k_{\parallel}^2}{\gamma\kappa} & 0 & 0 & \dfrac{\gamma-1}{\alpha\gamma\kappa} & \dfrac{\gamma-1}{\alpha\gamma\kappa} & 0\\ 0 & 0 & 0 & 1 & 0 & 0\\ 0 & \dfrac{\alpha c^2 s}{c^2+s\gamma\Gamma_v} & \dfrac{\gamma s(s+\nu k_{\parallel}^2)}{c^2+s\gamma\Gamma_v} & 0 & 0 & -\dfrac{c^2+s\gamma(\Gamma_v-\nu)}{c^2+s\gamma\Gamma_v}\\ 0 & 0 & 0 & 0 & 0 & 1\\ -\dfrac{\alpha c^2k_{\parallel}^2}{\gamma\nu} & 0 & 0 & \dfrac{k_{\parallel}^2[c^2+s\gamma(\Gamma_v-\nu)]}{\gamma\nu s} & \dfrac{\gamma s^2+k_{\parallel}^2(c^2+s\gamma\Gamma_v)}{\gamma\nu s} & 0 \end{bmatrix} \tag{2.12}$$

and

$$\vec{f}(z)=\begin{bmatrix} 0 \\ -\frac{1}{\gamma\kappa}\delta T(z) \\ 0 \\ \frac{c^2}{\rho_0(c^2+s\gamma\Gamma_v)}\frac{d\delta\rho(z)}{dz}-\frac{\gamma s}{c^2+s\gamma\Gamma_v}u_z(z) \\ 0 \\ -\frac{1}{\nu}\phi(z)-\frac{c^2k_{\|}^2}{\rho_0\gamma\nu s}\delta\rho(z) \end{bmatrix}, \tag{2.13}$$

where $\delta T(z)$, $\delta\rho(z)$, $u_z(z)$, and $\phi(z)$ are the initial values of fluctuations for a given value of $k_{\|}$.

The general solution of Eq. (2.11) is

$$\vec{F}(z)=e^{\underline{M}z}\vec{C}+\int_{z_0}^{z}dz'e^{\underline{M}(z-z')}\vec{f}(z')\ . \tag{2.14}$$

Thus, it is necessary to find the eigenvalues and eigenvectors of the matrix $\underline{M}$. There are three pairs of eigenvalues, denoted here by $\pm\lambda_i$, such that

$$\lambda_i=(k_{\|}^2-x_i)^{1/2}\ , \tag{2.15}$$

where

$$x_{1,2}=-\frac{s}{2\kappa(c^2+s\gamma\Gamma_v)}\{c^2+s(\Gamma_v+\gamma\kappa)\mp[(c^2+s\Gamma_v+s\gamma\kappa)^2-4s\kappa(c^2+s\gamma\Gamma_v)]^{1/2}\}\ , \tag{2.16a}$$

$$x_3=-\frac{s}{\nu}\ . \tag{2.16b}$$

Let $\underline{A}$ denote the matrix of eigenvectors of $\underline{M}$ and let $\underline{A}^{-1}$ be its inverse; both $\underline{A}$ and $\underline{A}^{-1}$ are given explicitly in Appendix A. Then

$$\underline{D}(z)\equiv\underline{A}^{-1}e^{\underline{M}z}\underline{A} \tag{2.17}$$

is the diagonal matrix with elements $\exp(\pm\lambda_i z)$, and from Eq. (2.14)

$$\vec{F}(z)=\underline{A}\,\underline{D}(z)\vec{c}+\int_{z_0}^{z}dz'\underline{A}\,\underline{D}(z-z')\underline{A}^{-1}\vec{f}(z')\ . \tag{2.18}$$

Equation (2.18) is the general solution of Eqs. (2.6)—(2.8), with the vector $\vec{c}$ to be determined from the boundary conditions. Using Eq. (2.18) the dynamic correlation function between any two fluctuating variables can be determined in terms of the appropriate static correlation functions. Since the quantity of experimental interest is the dynamic structure factor, the remainder of this paper is devoted to explicit calculations of the frequency-dependent density autocorrelation function for different choices of interfacial energy and tangential momentum transport.

III. DENSITY AUTOCORRELATION FUNCTION IN A FLUID LAYER

The calculation of the dynamic density autocorrelation function $\langle\tilde{\rho}(k_{\|},z;s)\delta\rho(z)\rangle$ can be simplified considerably by noting that, in equilibrium, the static correlation functions $\langle\delta\rho u_z\rangle=\langle\delta\rho\phi\rangle=\langle\delta\rho\delta T\rangle=0$. Hence, without any loss in generality one may set

$$\delta T(z)=u_z(z)=\phi(z)=0\ ;$$

this simplifies the vector of initial values $\vec{f}$, which now has only two nonvanishing components.

Using expressions for $\underline{A}$ and $\underline{A}^{-1}$ from Appendix A, the solutions for the fluctuating hydrodynamic variables are found to be

$$\tilde{T}=A_1[c_1\psi_1(z)+c_2\theta_1(z)]+A_2[c_3\psi_2(z)+c_4\theta_2(z)]+T_p(z)\ , \tag{3.1}$$

$$\tilde{u}_z=-c_1P_1\theta_1(z)-c_2S_1\psi_1(z)-c_3P_2\theta_2(z)-c_4S_2\psi_2(z)+c_5S_3\psi_3(z)+c_6P_3\theta_3(z)+u_p(z)\ , \tag{3.2}$$

$$\tilde{\phi}=k_{\|}^2[c_1\psi_1(z)+c_2\theta_1(z)+c_3\psi_2(z)+c_4\theta_2(z)]-c_5\theta_3(z)-c_6\psi_3(z)+\phi_p(z)\ , \tag{3.3}$$

where, for $i=1,2,3$,

$$\psi_i(z)\equiv\frac{\cosh(\lambda_i z)}{\cosh(\lambda_i L/2)}\ ,$$

$$\theta_i(z)\equiv\frac{\sinh(\lambda_i z)}{\sinh(\lambda_i L/2)}\ ,$$

$$R_i \equiv \tanh(\lambda_i L/2) ,$$

and, for $i=1,2$,

$$P_i \equiv \lambda_i R_i ,$$

$$S_i \equiv \lambda_i / R_i ,$$

and

$$P_3 \equiv R_3/\lambda_3 ,$$

$$S_3 \equiv 1/(\lambda_3 R_3) . \tag{3.4}$$

In addition,

$$T_p(z) = -A_0 A_1 A_2 \int_{-L/2}^{z} dz' \delta\rho(z') \{\lambda_2 x_1 \sinh[\lambda_1(z-z')] - \lambda_1 x_2 \sinh[\lambda_2(z-z')]\} , \tag{3.5a}$$

$$u_p(z) = A_0 \lambda_1 \lambda_2 \int_{-L/2}^{z} dz' \delta\rho(z') \{A_2 x_1 \cosh[\lambda_1(z-z')] - A_1 x_2 \cosh[\lambda_2(z-z')]\} , \tag{3.5b}$$

$$\phi_p(z) = -A_0 k_{\|}^2 \int_{-L/2}^{z} dz' \delta\rho(z') \{A_2 \lambda_2 x_1 \sinh[\lambda_1(z-z')] - A_1 \lambda_1 x_2 \sinh[\lambda_2(z-z')]\} , \tag{3.5c}$$

where

$$A_0 \equiv \frac{c^2}{\rho_0 \lambda_1 \lambda_2 (A_2 x_1 - A_1 x_2)(c^2 + s\gamma\Gamma_v)} , \tag{3.6a}$$

and, for $i=1,2$,

$$A_i \equiv -\frac{(\gamma-1)}{\alpha} \frac{x_i}{s+\gamma\kappa x_i} . \tag{3.6b}$$

Therefore, from Eq. (2.5), the solution for density fluctuations is

$$s\tilde{\rho} = -\rho_0 x_1 [c_1 \psi_1(z) + c_2 \theta_1(z)] - \rho_0 x_2 [c_3 \psi_2(z) + c_4 \theta_2(z)] + \frac{s\gamma\Gamma_v}{c^2 + s\gamma\Gamma_v} \delta\rho(z)$$

$$+ A_0 \rho_0 \int_{-L/2}^{z} dz' \delta\rho(z') \{A_2 \lambda_2 x_1^2 \sinh[\lambda_1(z-z')] - A_1 \lambda_1 x_2^2 \sinh[\lambda_2(z-z')]\} , \tag{3.7}$$

where the coefficients c_i depend on the boundary conditions for the variables $\tilde{T}$, and $\tilde{u}_z$, and $\tilde{\phi}$.

Since the dynamic structure factor is the correlation function of the Fourier modes of the density fluctuations, it is convenient to represent their initial values in a Fourier series

$$\delta\rho(z) = \sum_{n=-\infty}^{\infty} \delta\rho(n) e^{i(2\pi n/L)z} ; \tag{3.8}$$

this representation is valid for all z in $(-L/2, L/2)$. Let $\tilde{\rho}(n,s)$ denote the projection of $\tilde{\rho}(k_{\|},z;s)$ on the nth Fourier mode; i.e.,

$$\tilde{\rho}(n,s) \equiv \frac{1}{L} \int_{-L/2}^{L/2} dz\, e^{-i(2\pi n/L)z} \tilde{\rho}(k_{\|},z;s) . \tag{3.9}$$

Also let

$$c_i \equiv \tfrac{1}{2} A_0 \sum_{n=-\infty}^{\infty} \delta\rho(n) Q_i(n) \tag{3.10}$$

and

$$k^2 = k_{\|}^2 + k_{\perp}^2 \equiv k_{\|}^2 + \left[\frac{2\pi n}{L}\right]^2 . \tag{3.11}$$

Then, it follows from Eq. (3.7) that

$$\tilde{\rho}(n,s) = S_\infty(\vec{k},s)\delta\rho(n) + \frac{1}{sL} \sum_{n'=-\infty}^{\infty} S_L(\vec{k},\vec{k}',s)\delta\rho(n') , \tag{3.12}$$

where

$$S_\infty(\vec{k},s) = \frac{s^2 + s(\Gamma_v + \gamma\kappa)k^2 + (1-1/\gamma)c^2 k^2 + \gamma\kappa\Gamma_v k^4}{s^3 + s^2(\Gamma_v + \gamma\kappa)k^2 + s(c^2 + \gamma\kappa\Gamma_v k^2)k^2 + \kappa c^2 k^4} , \tag{3.13}$$

$$S_L(\vec{k},\vec{k}',s) = \tfrac{1}{2} A_0 \rho_0 [x_1 I_1(\vec{k}) Z_1(\vec{k},\vec{k}') - x_2 I_2(\vec{k}) Z_2(\vec{k},\vec{k}')] , \tag{3.14}$$

$$I_i(\vec{k}) = \frac{2(-1)^n}{k^2 - x_i} , \tag{3.15}$$

$$Z_1(\vec{k},\vec{k}') = \frac{A_2 \lambda_2 x_1 R_1}{1 - R_1^2} I_1(\vec{k}')[\lambda_1^2 - k_\perp k_\perp' + i(k_\perp + k_\perp')P_1] - P_1 Q_1(n') - i k_\perp Q_2(n') , \tag{3.16a}$$

$$Z_2(\vec{k},\vec{k}')=\frac{A_1\lambda_1 x_2 R_2}{1-R_2^2}I_2(\vec{k})[\lambda_2^2-k_\perp k_\perp'+i(k_\perp+k_\perp')P_2]+P_2Q_3(n')+ik_\perp Q_4(n') . \quad (3.16b)$$

It is clear from Eq. (3.12) that there exist dynamic correlations between Fourier modes with different values of $k_\perp$, and the appropriate density correlation functions are

$$\langle\tilde{\rho}(n,s)\delta\rho^*(n')\rangle=S_\infty(\vec{k},s)S(\vec{k},\vec{k}')+\frac{1}{sL}\sum_{k_\perp''}S_L(\vec{k},\vec{k}'',s)S(\vec{k}'',\vec{k}') , \quad (3.17)$$

where the static correlation function is

$$S(\vec{k},\vec{k}')\equiv\langle\delta\rho(n)\delta\rho^*(n')\rangle . \quad (3.18)$$

The dynamic structure factor

$$S(\vec{k},\vec{k}',\omega)=\frac{1}{\pi}\operatorname{Re}\langle\tilde{\rho}(n,s=i\omega)\delta\rho^*(n')\rangle \quad (3.19)$$

can, therefore, be determined from Eq. (3.17). In the infinite fluid, the static correlation function is diagonal; i.e.,

$$S(\vec{k},\vec{k}')=S(\vec{k})\delta_{\vec{k},\vec{k}'} \quad (3.20)$$

so that in the limit $L\to\infty$

$$\frac{S(\vec{k},\vec{k}',\omega)}{S(\vec{k})}=\frac{1}{\pi}\operatorname{Re}S_\infty(\vec{k},s=i\omega)\delta_{\vec{k},\vec{k}'} , \quad (3.21)$$

and the dynamic structure factor is diagonal. The normal hydrodynamic modes of the fluid are determined from the poles of the dynamic structure factor; it is easy to see from Eq. (3.13) that there are three poles in $S_\infty(\vec{k},\omega)$, with dispersion relation in the limit of small k

$$\omega=i\kappa k^2 \quad (3.22a)$$

for diffusive heat mode, and

$$\omega=\pm ck+i\Gamma k^2 \quad (3.22b)$$

for two propagating sound modes, where

$$\Gamma=\tfrac{1}{2}[\Gamma_v+(\gamma-1)\kappa] \quad (3.23)$$

is the attenuation coefficient for bulk sound modes.

Even though Eq. (3.17) is the exact density autocorrelation function in a fluid layer, it cannot be evaluated explicitly in this form, since the static correlation functions in the presence of interfaces are not known. Here, we assume that the static structure factor is diagonal [satisifes Eq. (3.20)] even for finite values of L. We expect that in fluid layers away from any critical points, the off-diagonal elements in $S(\vec{k},\vec{k}')$ are negligible except for very large (nonhydrodynamic) values of k; for k^{-1} on the order of intermolecular distances, the differences between the fluid molecule-molecule interaction and molecule-solid interaction may become significant. Therefore, for small values of k, we expect that the dynamic structure factor is of the form

$$\frac{S(\vec{k},\vec{k}',\omega)}{S(\vec{k}')}=\frac{1}{\pi}\operatorname{Re}\left[S_\infty(\vec{k},s=i\omega)\delta_{\vec{k},\vec{k}'}-\frac{i}{\omega L}S_L(\vec{k},\vec{k}',s=i\omega)\right] ; \quad (3.24)$$

this expression is evaluated in the remainder of the paper. However, even if the static structure factor is diagonal, the dynamic structure factor has off-diagonal elements whose amplitude vanishes as $L\to\infty$. While the assumption of diagonal structure factor may affect the amplitudes, it does not change the nature of the normal modes of the fluid layer which are given by the poles of $S_\infty(\vec{k},s)$ and $S_L(\vec{k},\vec{k}',s)$. The analytic structure of S_L is much more complicated than that of S_∞ and depends on the boundary conditions through functions Q_i. In the following sections, it is shown that Q_i's may have poles corresponding to interfacial propagating modes which are distinct from the bulk sound modes.

IV. DYNAMICS OF FLUCTUATIONS IN SOLID BOUNDARIES AND INTERFACIAL TRANSPORT

In the study of hydrodynamic properties of fluids confined by solid boundaries, the acoustic excitations of the solid are usually neglected; i.e., the acoustic impedance of the interface is assumed to be infinite. With this assumption, and in the absence of interfacial mass transport, the normal component of velocity vanishes at interfaces

$$\tilde{u}_z=0 , \quad z=\pm L/2 . \quad (4.1)$$

More interesting is the question of tangential momentum transport. It is well established experimentally that for fluid-solid interfaces in the limit of vanishing frequency this transport is maximum, leading to the so-called stick boundary conditions on tangential components of velocity; i.e.,

$$\tilde{\phi}=0\ ,\quad z=\pm L/2\ . \tag{4.2}$$

It has been argued that this effect is caused by the surface roughness, which leads to the perfectly diffuse scattering of the fluid molecules from the solid walls.[5,6] It would be very interesting to determine (by careful experimentation with interfaces of different roughness, over a wide frequency range) whether there exist conditions for which the tangential momentum transport is less than maximum resulting in a finite slip at the interface. In the absence of tangential momentum transport, the tangential stress is continuous across the interface; i.e.,

$$\frac{d\tilde{\phi}}{dz}=0\ ,\quad z=\pm L/2\ . \tag{4.3}$$

In this paper only the extreme limits of stick and slip boundary conditions on the velocity field will be considered.

We analyze in greater detail effects of temperature fluctuations in solid boundaries on the dynamic structure factor of a fluid layer. The dynamics of these fluctuations is governed by the heat conduction equation

$$\frac{\partial \delta T_s}{\partial t}=\kappa_s \nabla^2 \delta T_s\ , \tag{4.4}$$

where $\kappa_s=\lambda_s/(\rho_s C_{ps})$ is the thermal diffusivity, and subscript s refers to the solid. After taking the Laplace transform in time and the Fourier transform in the xy plane, Eq. (4.4) becomes

$$\frac{d^2\tilde{T}_s}{dz^2}-\left[k_{\|}^2+\frac{s}{\kappa_s}\right]\tilde{T}_s=-\frac{1}{\kappa_s}\delta T_s(z)\ , \tag{4.5}$$

where $\delta T_s(z)$ is the initial value of the temperature fluctuation in the solid. Since $\langle \delta\rho\delta T_s\rangle$ vanishes in equilibrium, $\delta T_s(z)$ can be set to zero without loss in generality. Then the solutions of Eq. (4.5) which vanish as $z\rightarrow\pm\infty$ are

$$\tilde{T}_s=\begin{cases} a_1 e^{-\lambda_4 z}, & L/2\le z<\infty \\ a_2 e^{\lambda_4 z}, & -\infty<z\le -L/2 \end{cases} \tag{4.6}$$

where

$$\lambda_4\equiv\left[k_{\|}^2+\frac{s}{\kappa_s}\right]^{1/2}\ . \tag{4.7}$$

Assuming the continuity of the heat and entropy fluxes across the interfaces, one has that at $z=\pm L/2$

$$\tilde{T}=\tilde{T}_s\ ,$$

$$\lambda\frac{d\tilde{T}}{dz}=\lambda_s\frac{d\tilde{T}_s}{dz}\ . \tag{4.8}$$

This leads to the boundary condition on the fluid temperature

$$\frac{d\tilde{T}}{dz}\pm\delta_T(k_{\|},s)\tilde{T}=0\ ,\quad z=\pm L/2\ , \tag{4.9}$$

where

$$\delta_T(k_{\|},s)=\frac{\rho_s C_{ps}\kappa_s}{\rho_0 C_p \kappa}\lambda_4\ . \tag{4.10}$$

V. DYNAMIC STRUCTURE FACTOR FOR STICK BOUNDARY CONDITIONS ON THE VELOCITY FIELD

For stick boundary conditions, Eq. (4.2), together with boundary conditions on the normal velocity component, Eq. (4.1), and on the temperature, Eq. (4.9), the coefficients c_i are determined from the solution of

$$\underline{G}\vec{c}+\vec{g}=0\ , \tag{5.1}$$

where

$$\underline{G}=\begin{bmatrix} -A_1(P_1+\delta_T) & A_1(S_1+\delta_T) & -A_2(P_2+\delta_T) & A_2(S_2+\delta_T) & 0 & 0 \\ A_1(P_1+\delta_T) & A_1(S_1+\delta_T) & A_2(P_2+\delta_T) & A_2(S_2+\delta_T) & 0 & 0 \\ P_1 & -S_1 & P_2 & -S_2 & S_3 & -P_3 \\ -P_1 & -S_1 & -P_2 & -S_2 & S_3 & P_3 \\ k_{\|}^2 & -k_{\|}^2 & k_{\|}^2 & -k_{\|}^2 & 1 & -1 \\ k_{\|}^2 & k_{\|}^2 & k_{\|}^2 & k_{\|}^2 & -1 & -1 \end{bmatrix}, \tag{5.2}$$

$$\vec{g}=\begin{bmatrix}0\\g_1\\0\\g_2\\0\\g_3\end{bmatrix}=\begin{bmatrix}0\\ \left.\frac{dT_p}{dz}\right|_{z=L/2}+\delta_T T_p(L/2)\\0\\u_p(L/2)\\0\\\phi_p(L/2)\end{bmatrix}, \tag{5.3}$$

and the various quantities entering in Eqs. (5.2) and (5.3) are defined in Eqs. (3.4)–(3.6). The solutions for the c_i's are given in Appendix B. After some tedious algebra, the L-dependent contribution to the dynamic density autocorrelation function is found to be

$$S_L(\vec{k},\vec{k}',s)=\frac{2(-1)^{n+n'}c^2}{(A_2x_1-A_1x_2)(c^2+s\gamma\Gamma_v)}\left[\frac{A_2x_1Y_1(k_\perp,k'_\perp)}{k^2-x_1}-\frac{A_1x_2Y_2(k_\perp,k'_\perp)}{k^2-x_2}\right], \tag{5.4}$$

where

$$Y_1=\frac{P_1x_1}{(k')^2-x_1}+\frac{P_1W_1}{T(U)}+\frac{k_\perp k'_\perp W_2}{T(V)}, \tag{5.5}$$

$$Y_2=\frac{P_2x_2}{(k')^2-x_2}+\frac{P_2W_3}{T(U)}+\frac{k_\perp k'_\perp W_4}{T(V)}, \tag{5.6}$$

$$W_1=\frac{P_1x_1[A_2(P_2+\delta_T)-A_1U_2]}{(k')^2-x_1}-\frac{A_1P_2x_2(\delta_T+k_{\parallel}^2P_3)}{(k')^2-x_2}, \tag{5.7}$$

$$W_2=\frac{x_1[A_2(S_2+\delta_T)-A_1V_2]}{(k')^2-x_1}-\frac{A_1x_2(\delta_T+k_{\parallel}^2S_3)}{(k')^2-x_2}, \tag{5.8}$$

$$W_3=\frac{A_2P_1x_1(\delta_T+k_{\parallel}^2P_3)}{(k')^2-x_1}-\frac{P_2x_2[A_1(P_1+\delta_T)-A_2U_1]}{(k')^2-x_2}, \tag{5.9}$$

$$W_4=\frac{A_2x_1(\delta_T+k_{\parallel}^2S_3)}{(k')^2-x_1}-\frac{x_2[A_1(S_1+\delta_T)-A_2V_1]}{(k')^2-x_2}, \tag{5.10}$$

$$T(U)=A_1U_2(P_1+\delta_T)-A_2U_1(P_2+\delta_T), \tag{5.11}$$

$$T(V)=A_1V_2(S_1+\delta_T)-A_2V_1(S_2+\delta_T), \tag{5.12}$$

$$U_i\equiv P_i-k_{\parallel}^2P_3, \tag{5.13}$$

$$V_i\equiv S_i-k_{\parallel}^2S_3. \tag{5.14}$$

Despite the complicated appearance, it is easy to check from Eqs. (5.4)–(5.10) that the matrix $S_L(\vec{k},\vec{k}',s)$ is symmetric.

The normal hydrodynamic modes of the fluid layer are found from the poles of the dynamic structure factor; these modes do not include the diffusive shear modes from which density fluctuations are decoupled. The poles of $S_\infty(\vec{k},s)$ are discussed in Sec. III. Here we consider only the analytic structure of $S_L(\vec{k},\vec{k}',s)$.

A. Bulk sound modes

The dispersion relation for these modes is determined from

$$K^2=x_1,\quad K=k,k'. \tag{5.15}$$

From Eq. (2.16a), the dispersion relation in the limit of small K is

$$\omega=\pm cK+i\Gamma K^2, \tag{5.16}$$

where Γ is the bulk sound attenuation coefficient defined in Eq. (3.23). It follows from Eqs. (2.15) and (5.15) that

$$\lambda_1=i\frac{2\pi N}{L},\quad N=n,n'$$

and, therefore,

$$R_1=\tanh(\tfrac{1}{2}\lambda_1L)=0.$$

Thus, $P_1=0$ and $S_1=\infty$, so that the amplitudes of these sound modes vanish unless $k_\perp=k'_\perp$. In the limit of small k the contribution of S_L to the diagonal part of the dynamic structure factor cancels that of S_∞; i.e., the ordinary Brillouin peaks disappear in sufficiently thin fluid layers. In practice, the amplitudes of the Brillouin peaks remain finite unless L is small enough so that the condition

$$\tfrac{1}{4}(k_\perp L)\left[\frac{2\Gamma k}{c}\right]^2\left[\frac{k}{k_\perp}\right]^2 \ll 1 \tag{5.17}$$

is satisfied. Therefore, for typical fluid parameters and $k_\parallel \sim 10^5$ cm^{-1}, the Brillouin peaks disappear from the dynamic structure factor for $L \ll 0.1$ cm for $k_\perp \sim k_\parallel$, or for $L \ll 10^{-2}$ cm for $k_\perp \ll k_\parallel$.

B. Bulk heat modes

The dispersion relation for these modes is determined from

$$K^2 = x_2, \quad K = k, k' . \tag{5.18}$$

From Eq. (2.16a), the dispersion relation in the limit of small K is

$$\omega = i\kappa K^2 . \tag{5.19}$$

In this case, it is

$$\lambda_2 = i\frac{2\pi N}{L}, \quad N = n, n'$$

so that $P_2 = 0$ and $S_2 = \infty$. As before, these modes contribute only to the diagonal part of the dynamic structure factor and for sufficiently small values of L such that

$$\tfrac{1}{4}(k_\perp L)\frac{(\gamma-1)\kappa\,|\,\Gamma_v-\kappa\,|}{c^2}\frac{k^4}{k_\perp^2} \ll 1 ; \tag{5.20}$$

this contribution cancels that from S_∞ and the Rayleigh peak disappears.

C. Waveguide sound modes

In this case the dispersion relation is determined from

$$P_1 = \infty . \tag{5.21}$$

Since

$$P_1 = \lambda_1 \tanh(\tfrac{1}{2}\lambda_1 L) = \frac{4\lambda_1^2}{L}\sum_{m=0}^{\infty}\frac{1}{\lambda_1^2 + (2m+1)^2\pi^2/L^2} , \tag{5.22}$$

there is an infinite number of poles of P_1, which in the limit of small values of $K(m)$ occur for

$$\omega = \pm cK(m) + i\Gamma K^2(m) , \tag{5.23}$$

where

$$K^2(m) = k_\parallel^2 + \frac{(2m+1)^2\pi^2}{L^2} \equiv k_\parallel^2 + k_m^2 . \tag{5.24}$$

These waveguide sound modes appear because they are not orthogonal to modes with $k_\perp = 2\pi m/L$, chosen as the basis in representing the density fluctuations in a Fourier series.[7] Therefore, they are present independently of values of $k_\perp$ and $k'_\perp$. The amplitudes of these modes, however, vanish for sufficiently small values of L, given by condition (5.17) with $k_\perp$ replaced by k_m. For larger values of L, the amplitudes are finite and proportional to $(k_\perp^2 - k_m^2)^{-1}$ and $(k_\perp'^2 - k_m^2)^{-1}$. Hence, these waveguide modes are most pronounced in the vicinity of the infinite fluid Brillouin peaks.

D. Waveguide heat modes

The dispersion relation is determined from

$$P_2 = \infty . \tag{5.25}$$

Again, there is an infinite number of poles of P_2 which in the limit of small values of $K(m)$ occur for

$$\omega = i\kappa K^2(m) . \tag{5.26}$$

These diffusive heat modes are present independently of values of $k_\perp$ and $k'_\perp$; their amplitudes vanish for sufficiently small values of L, given by condition (5.20) with $k_\perp$ replaced by k_m. For larger values of L, the amplitudes are finite, but since these modes have zero shifts, they are superposed on the central Rayleigh peak and are, therefore, unobservable.

E. Interfacial modes

Thus, it is seen that for sufficiently small values of L, the amplitudes of the ordinary sound and heat modes vanish, and the total intensity of density fluctuations is in the new interfacial modes whose dispersion relation is given by the solutions of

$$T(U) = 0 \quad \text{or} \quad T(V) = 0 . \tag{5.27}$$

In general, the dispersion relation for these modes depends on the component of wave vector parallel to the boundaries $k_\parallel$ and on the height of the fluid layer L. While the transcendental equations (5.27) can be solved numerically for any values of L, one can find analytic results for the dispersion relation in the limit of L sufficiently large so that

$$\mathrm{Re}(\tfrac{1}{2}\lambda_i L) \gg 1, \quad i = 1,2,3 \tag{5.28}$$

and

$$P_i \approx S_i \approx \lambda_i, \quad i=1,2$$
$$P_3 \approx S_3 \approx 1/\lambda_3 , \tag{5.29}$$
$$U_i \approx V_i \approx \lambda_i - k_{\parallel}^2 \lambda_3 \equiv \tilde{U}_i .$$

Then, $T(U) \approx T(V)$ and the dispersion relation is determined from

$$A_1 \tilde{U}_2(\lambda_1+\delta_T) = A_2 \tilde{U}_1(\lambda_2+\delta_T) , \tag{5.30}$$

where δ_T is given in Eq. (4.10). In the limit of small $k_{\parallel}$, the dispersion relation is

$$\omega = \pm ck_{\parallel} + i[\Gamma + \Lambda(k_{\parallel})]k_{\parallel}^2 , \tag{5.31}$$

where

$$[2\Lambda(k_{\parallel})]^{1/2} = \sqrt{2\Gamma'} - (\gamma-1)\sqrt{\kappa}\left\{\left[\frac{\rho_s C_{ps}}{\rho_0 C_p}\right]\left[\frac{\kappa_s}{\kappa}\left[1 \mp \frac{ik_{\parallel}\kappa_s}{c}\right]\right]^{1/2} + 1\right\}^{-1} , \tag{5.32}$$

and

$$\Gamma' = \tfrac{1}{2}[\sqrt{\nu} + (\gamma-1)\sqrt{\kappa}]^2 . \tag{5.33}$$

Since $\Lambda(k_{\parallel})$ is explicitly complex, both the shifts and the widths of the new peaks in the dynamic structure factor depend on the ratio of thermal diffusivities of the solid and fluid. In the limit $\kappa_s/\kappa \gg 1$, so that $\kappa_s k_{\parallel}/c \gg 1$,

$$\omega \cong \pm ck_{\parallel}\left[1 + (\gamma-1)\left[\frac{\Gamma' k_{\parallel}}{c}\right]^{1/2} \frac{\rho_0 C_p}{\rho_s C_{ps}} \frac{\kappa}{\kappa_s}\right] + i\left[\Gamma + \Gamma' - (\gamma-1)\left[\frac{\Gamma' c}{k_{\parallel}}\right]^{1/2}\left[\frac{\rho_0 C_p}{\rho_s C_{ps}}\right]\frac{\kappa}{\kappa_s}\right]k_{\parallel}^2 , \tag{5.34}$$

and in the limit $\kappa_s/\kappa \to \infty$ (perfectly conducting solid boundaries) the dispersion relation becomes

$$\omega = \pm ck_{\parallel} + i(\Gamma + \Gamma')k_{\parallel}^2 . \tag{5.35}$$

In the opposite limit of small thermal conductivity of the boundaries, $\kappa_s/\kappa \ll 1$,

$$\omega = \pm ck_{\parallel} + i\left[\Gamma + \tfrac{1}{2}\nu + (\gamma-1)(\nu\kappa_s)^{1/2}\frac{\rho_s C_{ps}}{\rho_0 C_p}\right]k_{\parallel}^2 . \tag{5.36}$$

Thus, the effect of finite thermal conductivity on the position of the new peaks is most pronounced for $1 \ll \kappa_s/\kappa < \infty$. Then the effective speed of the new modes depends on $\sqrt{k_{\parallel}}$. In the extreme limits ($\kappa_s/\kappa \to \infty$ or $\kappa_s/\kappa \to 0$), these new modes differ from the ordinary bulk sound modes only in that their dispersion relation is independent of $k_{\perp}$ and $k_{\perp}'$, and their attenuation is enhanced. The physical origin of the new modes is clear. Only the component of the sound modes propagating parallel to the interfaces experiences additional shear created by the sticky boundaries. This accounts for the appearance of shear viscosity ν in $\Lambda(k_{\parallel})$. There can also be additional dissipation due to heat conduction between the fluid and solid walls if the sound is not isothermal ($\gamma \neq 1$); hence, the appearance of κ and κ_s in $\Lambda(k_{\parallel})$. Note that, for thermally insulating boundaries ($\kappa_s/\kappa \to 0$), it is seen from Eq. (5.36) that the enhancement of attenuation is due only to additional shear and only ν appears in $\Lambda(k_{\parallel})$.

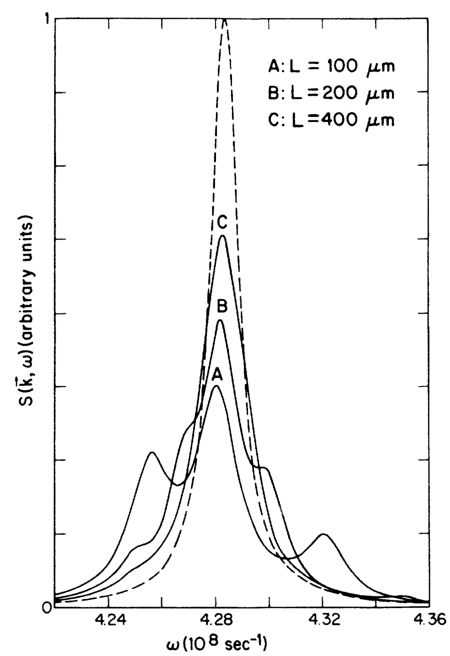

FIG. 1. Dynamic structure factor $S(\vec{k},\vec{k},\omega)$, for a fluid layer with stick boundary conditions, near the Brillouin frequency for three values of the layer height L. Fluid parameters are those of argon at 85 K: $\kappa = 2.3\times10^{-2}$ cm^2/sec, $\nu = \zeta = 9\times10^{-3}$ cm^2/sec, $\gamma = 2.2$, $c = 8.5\times10^4$ cm/sec. In addition, $\rho_0 C_p = \rho_s C_{ps}$ is assumed and $\kappa_s/\kappa = 10^{-3}$. Components of the wave vector are $k_{\parallel} = 5\times10^3$ cm^{-1}, $k_{\perp} = 2\pi/L$. Brillouin peak of the infinite fluid (dashed curve) is shown for comparison.

The new modes are interfacial modes with amplitudes decreasing exponentially with the distance from the interfaces. This can be easily checked by taking the two solid boundaries to be of different materials. In this case, even for sufficiently large values of L, $T(U)\neq T(V)$. The breaking of the reflection symmetry lifts the degeneracy of the interfacial modes. For each distinct fluid-solid interface there are two propagating interfacial modes with dispersion relation given by Eq. (5.31) but with $\Lambda(k_{\parallel})$ determined from Eq. (5.32) with the parameters characteristic of the solid boundary.

For two identical solid boundaries, in the limit of L sufficiently large so that the condition (5.28) is satisfied, the contributions to the dynamic structure factor from the interfacial modes are

$$\frac{\Delta S^{\pm}(\vec{k},\vec{k}',\omega)}{S(\vec{k}')}=\frac{2(-1)^{n+n'}}{\gamma\pi(k_{\parallel}L)}\frac{1}{[(\Gamma+\mathrm{Re}\Lambda)k_{\parallel}^2]^2+(\omega\mp ck_{\parallel}+\mathrm{Im}\Lambda k_{\parallel}^2)^2}$$
$$\times\mathrm{Re}\left[\frac{k_{\parallel}^2\left[k_{\perp}k_{\perp}'\mp i\frac{2\Lambda}{c}k_{\parallel}^3\right][(\Gamma+\mathrm{Re}\Lambda)k_{\parallel}^2-i(\omega\mp ck_{\parallel}+\mathrm{Im}\Lambda k_{\parallel}^2)]\left[\mp i\frac{2\Lambda k_{\parallel}}{c}\right]^{1/2}}{\left[k_{\perp}^2\mp i\frac{2\Lambda}{c}k_{\parallel}^3\right]\left[(k_{\perp}')^2\mp i\frac{2\Lambda}{c}k_{\parallel}^3\right]}\right]. \tag{5.37}$$

For infinite thermal conductivity of the solid $\Lambda=\Gamma'$, and if $k_{\perp}^2\simeq k_{\perp}'^2\gg 2\Gamma' k_{\parallel}^3/c$, Eq. (5.37) reduces to

$$\frac{\Delta S^{\pm}(\vec{k},\vec{k}',\omega)}{S(\vec{k}')}=\frac{2(-1)^{n+n'}}{\gamma\pi k_{\parallel}L}\left[\frac{\Gamma' k_{\parallel}}{c}\right]^{1/2}\left[\frac{k_{\parallel}^2}{k_{\perp}k_{\perp}'}\right]\frac{(\Gamma+\Gamma')k_{\parallel}^2\mp(\omega\mp ck_{\parallel})}{[(\Gamma+\Gamma')k_{\parallel}^2]^2+(\omega\mp ck_{\parallel})^2}. \tag{5.38}$$

If, on the other hand, the solid boundaries are thermally insulating, the contributions to the dynamic structure factor from the interfacial modes are exactly as in Eq. (5.38) but with $\frac{1}{2}\nu$ replacing Γ'. Because of the presence of ω in the numerator of Eq. (5.38), even in the extreme limits of perfectly conducting or perfectly insulating solid boundaries, the line shapes are not Lorentzian. The contributions to the dynamic structure factor become significant for

$$k_{\parallel}L\sim\left[\frac{\Gamma' k_{\parallel}}{c}\right]^{1/2}\frac{k_{\parallel}^2}{k_{\perp}k_{\perp}'}. \tag{5.39}$$

Thus, as the separation of these peaks from the Brillouin peaks increases ($k_{\perp}$ increases) their amplitudes decrease. For $k_{\parallel}$ typical of light scattering experiments and transport coefficients characteristic of dense fluids, the contributions of interfacial modes become significant for $L\sim 100$ μm. For such small values of L, the amplitudes of the Rayleigh and Brillouin peaks decrease and the waveguide modes become important. In addition, $\mathrm{Re}(\frac{1}{2}\lambda_1 L)$ is no longer large compared to unity and the above approximate expressions no longer valid.

The dependence of the dynamic structure factor for a fluid layer on its height L and the ratio of thermal diffusivities of fluid and solid is illustrated in Figs. 1–3. The dynamic structure factor, shown in the vicinity of the infinite fluid Brillouin peak given for comparison, was evaluated using the exact expression for $S_L(\vec{k},\vec{k}',\omega)$ from Eq. (5.4). Since there is no new structure in the Rayleigh peak (only its amplitude changes as a function of L) it will not be considered any further. The fluid parameters are those of argon at 85 K chosen because of relatively large value of $\gamma=2.2$ in order to illustrate the effects of heat conduction between the fluid and solid. The dependence of the diagonal part of the dynamic structure factor on the layer height L, for $k_{\perp}=2\pi/L$ and $\kappa_s/\kappa=10^{-3}$, is shown in Fig. 1. It is seen that as L decreases, the amplitude of the Brillouin peak, centered at $\omega=ck$, decreases while the amplitudes of the waveguide modes, centered at $\omega=cK(m)$, in its vicinity increase. In addition, a new interfacial mode centered at $\omega\approx ck_{\parallel}$ appears. The dependence of the diagonal part of the dynamic structure factor on $k_{\perp}=2\pi n/L$ for $n=0,1,2$ and on the ratio of thermal diffusivities of the fluid and solid is shown in Fig. 2. For $k_{\perp}=0$, the interfacial peak is superposed on the Brillouin peak and only the amplitude and line shape of the resulting single peak are affected by the ratio of the thermal diffusivities. For $k_{\perp}=2\pi/L$, $L=100$ μm, the interfacial peak is well resolved only for solid boundaries of low thermal conductivity. This is not surprising since the additional dissipation due to heat conduction from fluid to solid of high thermal conductivity increases the width and decreases the amplitude of the interfacial peaks. Note that the amplitude of the Brillouin peak is reduced considerably; this also happens for $k_{\perp}=4\pi/L$. In this case, the interfacial peak is well

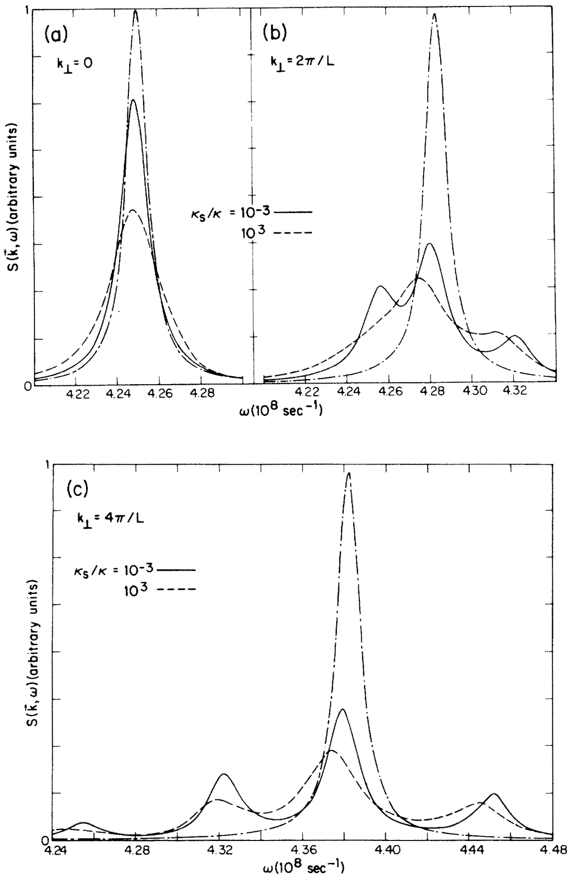

FIG. 2. Dynamic structure factor $S(\vec{k},\vec{k},\omega)$, for a fluid layer with stick boundary conditions, near the Brillouin frequency for $k_\perp=0$, $2\pi/L$, and $4\pi/L$, and $L=100$ μm. Other parameters are as in Fig. 1, but the solid curves pertain to poor thermal diffusivity of the solid ($\kappa_s/\kappa=10^{-3}$) while the dashed curves to high thermal diffusivity ($\kappa_s/\kappa=10^3$). Brillouin peak of the infinite fluid (dot-dashed curve) is shown for comparison.

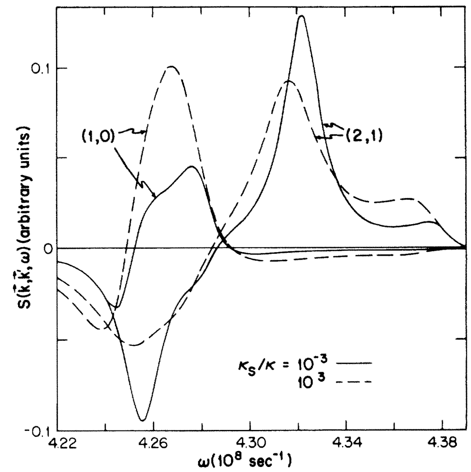

FIG. 3. Off-diagonal elements of the dynamic structure factor $S(\vec{k},\vec{k}\,',\omega)$, for a fluid layer with stick boundary conditions, near the Brillouin frequency for different values of $k_\perp=2\pi n/L$ and $k'_\perp=2\pi n'/L$ with $L=100$ μm. Curves are labeled (n,n'). Other parameters are as in Fig. 1, but the solid curves pertain to poor thermal diffusivity of the solid ($\kappa_s/\kappa=10^{-3}$), while dashed curves to high thermal diffusivity ($\kappa_s/\kappa=10^3$). Scale is set by the Brillouin peak of the infinite fluid with $k_\perp=k'_\perp=0$.

separated from the Brillouin peak, but, as was seen from Eq. (5.37), its amplitude is much smaller than that of the Brillouin peak in unbounded fluid. The waveguide modes are also clearly seen in Fig. 2(c).

The diagonal elements of the dynamic structure factor, shown in Figs. 1 and 2, are of direct experimental interest. The off-diagonal elements, which vanish in an unbounded fluid, are more difficult to probe experimentally. They are shown in Fig. 3 for different combinations of $k_\perp$ and $k'_\perp$. For the values of the parameters chosen here and if $|k_\perp-k'_\perp|=2\pi/L$ the amplitudes of various peaks are typically reduced by a factor of 10 from the amplitude of an infinite fluid Brillouin peak. As the separation between $k_\perp$ and $k'_\perp$ increases, the amplitudes decrease further. In addition, it should be noted that in contrast to the diagonal elements of $S(\vec{k},\vec{k}\,',\omega)$, which are non-negative, the off-diagonal elements can have any sign as is clearly seen in Fig. 3. As before, for thermally insulating solid boundaries, the interfacial peak is much better resolved from the waveguide modes than for boundaries of high thermal conductivity.

VI. DYNAMIC STRUCTURE FACTOR FOR SLIP BOUNDARY CONDITIONS ON THE VELOCITY FIELD

While the assumption of no tangential momentum transport across the fluid-solid interface is not physically correct, it is often used for mathematical simplicity, especially if the fluid is taken to be incompressible. In this section, we analyze the consequences of this assumption on the dynamics of equilibrium fluid fluctuations.

With boundary conditions given by Eqs. (4.1), (4.3), and (4.9), the coefficients c_i are determined from the solutions of

$$\underline{H}\vec{c}+\vec{h}=0\,, \tag{6.1}$$

where

$$\underline{H}=\begin{bmatrix} -A_1(P_1+\delta_T) & A_1(S_1+\delta_T) & -A_2(P_2+\delta_T) & A_2(S_2+\delta_T) & 0 & 0 \\ A_1(P_1+\delta_T) & A_1(S_1+\delta_T) & A_2(P_2+\delta_T) & A_2(S_2+\delta_T) & 0 & 0 \\ P_1 & -S_1 & P_2 & -S_2 & S_3 & -P_3 \\ -P_1 & -S_1 & -P_2 & -S_2 & S_3 & P_3 \\ -k_{\parallel}^2P_1 & k_{\parallel}^2S_1 & -k_{\parallel}^2P_2 & k_{\parallel}^2S_2 & -1/P_3 & 1/S_3 \\ k_{\parallel}^2P_1 & k_{\parallel}^2S_1 & k_{\parallel}^2P_2 & k_{\parallel}^2S_2 & -1/P_3 & -1/S_3 \end{bmatrix} \quad (6.2)$$

and, since $d\phi_p/dz=-k_{\parallel}^2u_p$,

$$\vec{h}^T=(0,g_1,0,g_2,0,-k_{\parallel}^2g_2) \quad (6.3)$$

with g_1 and g_2 defined in Eq. (5.3). The solutions for c_i's are given in Appendix C.

The L-dependent contribution to the dynamic structure factor for a fluid layer with slip boundary condition is

$$S_L(\vec{k},\vec{k}',s)=\frac{2(-1)^{n+n'}c^2}{(A_2x_1-A_1x_2)(c^2+s\gamma\Gamma_v)}\left[\frac{A_2x_1Y_1(k_\perp,k_\perp')}{k^2-x_1}-\frac{A_1x_2Y_2(k_\perp,k_\perp')}{k^2-x_2}\right], \quad (6.4)$$

where

$$Y_1=\frac{A_1W_1}{T(P)}+\frac{k_\perp k_\perp' W_2}{T(S)}, \quad (6.5)$$

$$Y_2=\frac{A_2W_1}{T(P)}-\frac{k_\perp k_\perp' W_3}{T(S)}, \quad (6.6)$$

$$W_1=P_1P_2\delta_T\left[\frac{x_1}{(k')^2-x_1}-\frac{x_2}{(k')^2-x_2}\right], \quad (6.7)$$

$$W_2=\frac{x_1[A_2(S_2+\delta_T)-A_1S_2]}{(k')^2-x_1}-\frac{A_1x_2\delta_T}{(k')^2-x_2}, \quad (6.8)$$

$$W_3=\frac{x_2[A_1(S_1+\delta_T)-A_2S_1]}{(k')^2-x_2}-\frac{A_2x_1\delta_T}{(k')^2-x_1}, \quad (6.9)$$

$$T(P)=A_1P_2(P_1+\delta_T)-A_2P_1(P_2+\delta_T), \quad (6.10)$$

$$T(S)=A_1S_2(S_1+\delta_T)-A_2S_1(S_2+\delta_T). \quad (6.11)$$

Again, it is easy to check that the matrix $S_L(\vec{k},\vec{k}',s)$ is symmetric.

As before, the normal hydrodynamic modes of the fluid layer with slip boundary conditions on the velocity field are found from the poles of the dynamic structure factor. The poles of $S_\infty(\vec{k},s)$ are independent of boundary conditions and are discussed in Sec. III. Therefore, only the analytic structure of $S_L(\vec{k},\vec{k}',s)$ is considered here. Its nature depends strongly on the values of the ratio of thermal diffusivities of the fluid and solid. Consider first the case of finite values of κ_s/κ; i.e., finite values of δ_T. Then the nature of the sound and heat modes, with dispersion relations given in Eqs. (5.16), (5.19), (5.23), and (5.26), as well as their amplitudes, is the same as in the case of stick boundary conditions on the velocity field. Therefore, the discussion of these modes in Sec. V applies here. Thus, for sufficiently small values of L and k, the amplitudes of the bulk sound and heat modes become negligible and the total intensity of density fluctuations is in the interfacial modes whose dispersion relation is now given by the solutions of

$$T(P)=0 \quad \text{or} \quad T(S)=0\,. \quad (6.12)$$

Analytic expressions for the dispersion relation and the amplitudes of interfacial modes can be obtained in the limit of L sufficiently large so that condition (5.28) is satisfied. Then $T(P)\simeq T(S)$ and the dispersion relation determined from

$$A_1\lambda_2(\lambda_1+\delta_T)=A_2\lambda_1(\lambda_2+\delta_T). \quad (6.13)$$

Again, the dispersion relation for the interfacial modes depends only on $k_{\parallel}$, and in the limit of small $k_{\parallel}$ is

$$\omega=\pm ck_{\parallel}+i[\Gamma+\Lambda_s(k_{\parallel})]k_{\parallel}^2, \quad (6.14)$$

where

$$[2\Lambda_s(k_{\parallel})]^{1/2}=(\gamma-1)\sqrt{\kappa}\left\{1-\left[\frac{\rho_sC_{ps}}{\rho_0C_p}\left[\frac{\kappa_s}{\kappa}\right]^{1/2}\left[1\mp i\frac{\kappa_sk_{\parallel}}{c}\right]^{1/2}+1\right]^{-1}\right\}. \quad (6.15)$$

It is seen that in the case of slip boundary conditions, the dispersion relation is the same as in the case of stick boundary conditions, but with Γ' evaluated for a vanishing shear viscosity. This is not surprising, since for slip boundary conditions there is no additional shear due to solid boundaries. The attenuation is enhanced relative to the bulk sound modes only because of additional dissipation due to heat conduction between the fluid and solid.

In the limit of large L [condition (5.28) satisfied] the contributions to the dynamic structure factor from the interfacial modes are again given by Eq. (5.37) but with $\Lambda(k_{\|})$ replaced by $\Lambda_s(k_{\|})$. Thus, these contributions become significant for

$$k_{\|}L \sim (\gamma-1)\left[\frac{\kappa k_{\|}}{2c}\right]^{1/2}\left[\frac{k_{\|}^2}{k_{\perp}k_{\perp}'}\right]; \tag{6.16}$$

they vanish if the sound is nearly isothermal, $\gamma \approx 1$. In general, for given fluid properties and thermal conductivity of solid boundaries, the interfacial modes are significant for lower values of L in the case of slip boundary conditions.

The analytic expressions given above, are not valid for thermally insulating solids; i.e., in the limit $\kappa_s/\kappa \to 0$ or $\delta_T \to 0$. In this case, the L-dependent contribution to the dynamic structure factor is simply

$$S_L(\vec{k},\vec{k}',s)=\frac{2(-1)^{n+n'}c^2k_{\perp}k_{\perp}'}{(A_2x_1-A_1x_2)(c^2+s\gamma\Gamma_v)}\left[\frac{A_1x_2^2P_2}{\lambda_2^2(k^2-x_2)[(k')^2-x_2]}-\frac{A_1x_1^2P_1}{\lambda_1^2(k^2-x_1)[(k')^2-x_1]}\right]. \tag{6.17}$$

Note, first of all, that the interfacial modes disappear since, due to lack of transport of either energy or tangential momentum across the interfaces, there are no additional mechanisms for dissipation. In addition, from Eq. (6.17) the sound modes with dispersion relation given in Eq. (5.16) contribute to dynamic structure factor in the limit of small k

$$\frac{\Delta S_1(\vec{k},\vec{k}',\omega)}{S(\vec{k}')}=-\frac{\delta_{n,n'}}{4\pi\gamma}\left[\frac{\Gamma k^2}{(\Gamma k^2)^2+(\omega-ck)^2}+\frac{\Gamma k^2}{(\Gamma k^2)^2+(\omega+ck)^2}\right]. \tag{6.18}$$

Therefore, on adding the appropriate contributions from $S_\infty(\vec{k},\omega)$ one finds that the intensity of the Brillouin peaks is reduced by a factor of 2. Similarly, the intensity of the Rayleigh peak is reduced by two since, from Eq. (6.17) the contribution of the heat mode with dispersion relation given in Eq. (5.19) is in the limit of small k

$$\frac{\Delta S_2(\vec{k},\vec{k}',\omega)}{S(\vec{k}')}=-\delta_{n,n'}\frac{(\gamma-1)}{2\pi\gamma}\frac{\kappa k^2}{(\kappa k^2)+\omega^2}, \tag{6.19}$$

i.e., $-2\Delta S_2(\vec{k},\vec{k}',\omega)$ is just the Rayleigh peak for an unbounded fluid. For thermally insulating solid boundaries, the amplitudes of the waveguide modes do not vanish even for small values of L; the fluid layer still acts as a waveguide since u_z vanishes at interfaces. For the sound modes with the dispersion relation given in Eq. (5.23), S_L contributes to both diagonal and off-diagonal elements of the dynamic structure factor

$$\frac{\Delta S_1^m(\vec{k},\vec{k}',\omega)}{S(\vec{k}')}=\sum_{m=0}^{\infty}\frac{4(-1)^{n+n'}k_{\perp}k_{\perp}'}{\pi\gamma L^2(k_{\perp}^2-k_m^2)[(k_{\perp}')^2-k_m^2]}\left[\frac{\Gamma K^2(m)}{[\Gamma K^2(m)]^2+[\omega-cK(m)]^2}+\frac{\Gamma K^2(m)}{[\Gamma K^2(m)]^2+[\omega+cK(m)]^2}\right], \tag{6.20}$$

where

$$K^2(m)=k_{\|}^2+k_m^2\equiv k_{\|}^2+\left[\frac{\pi(2m+1)}{L}\right]^2.$$

Similarly, for the heat modes with dispersion relation given in Eq. (5.26), S_L contributes

$$\frac{\Delta S_2^m(\vec{k},\vec{k}',\omega)}{S(\vec{k}')}=\sum_{m=0}^{\infty}\frac{8(\gamma-1)(-1)^{n+n'}k_{\perp}k_{\perp}'}{\pi\gamma L^2(k_{\perp}^2-k_m^2)[(k_{\perp}')^2-k_m^2]}\frac{\kappa K^2(m)}{[\kappa K^2(m)]^2+\omega^2}. \tag{6.21}$$

It is easy to show that

$$\int_{-\infty}^{\infty}d\omega\,\Delta S_i(\vec{k},\vec{k}',\omega)+\int_{-\infty}^{\infty}d\omega\,\Delta S_i^m(\vec{k},\vec{k}',\omega)=0 \tag{6.22}$$

so that the sum rule

$$\int_{-\infty}^{\infty} d\omega\, S(\vec{k},\vec{k}',\omega)=S(\vec{k})\delta_{n,n'} \tag{6.23}$$

is satisfied by the dynamic structure factor.

For slip boundary conditions on the velocity field, the dependence of the dynamic structure factor for a fluid layer on its height L and the ratio of thermal diffusivities of fluid and solid is illustrated in Figs. 4–6. $S(\vec{k},\vec{k}',\omega)$ is again shown in the vicinity of the infinite fluid Brillouin peak and was evaluated using the exact expression for $S_L(\vec{k},\vec{k}',s)$ from Eq. (6.4). The fluid parameters are again those of argon at 85 K. The dynamic structure factor in the case of slip boundary conditions and finite thermal conductivity of the solid is qualitatively similar to the one obtained in the case of stick boundary conditions. The dependence of $S(\vec{k},\vec{k},\omega)$ on the layer height L for $k_\perp=2\pi/L$ and $\kappa_s/\kappa=10^{-3}$ is shown in Fig. 4. For $L=100$ μm, the dependence of $S(\vec{k},\vec{k},\omega)$ on $k_\perp=2\pi n/L$ for $n=0,1,2$ and on the ratio κ_s/κ is shown in Fig. 5. The off-diagonal elements of $S(\vec{k},\vec{k}',\omega)$ are illustrated in Fig. 6 for various combinations of $k_\perp$ and $k'_\perp$; again the correlations between the Fourier modes with different values of $k_\perp$ can have either sign. The major difference between the dynamic structure factor for a fluid layer with slip boundary conditions and the one with stick boundary conditions is that the attenuation of the interfacial modes is higher in the latter case due to additional shear.

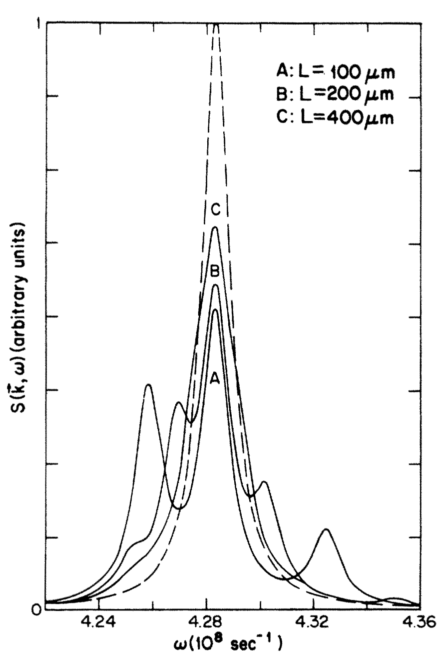

FIG. 4. Dynamic structure factor $S(\vec{k},\vec{k},\omega)$, for a fluid layer with slip boundary conditions, near the Brillouin frequency for three values of the layer height L. Parameters are as in Fig. 1. Brillouin peak of the infinite fluid (dashed curve) is shown for comparison.

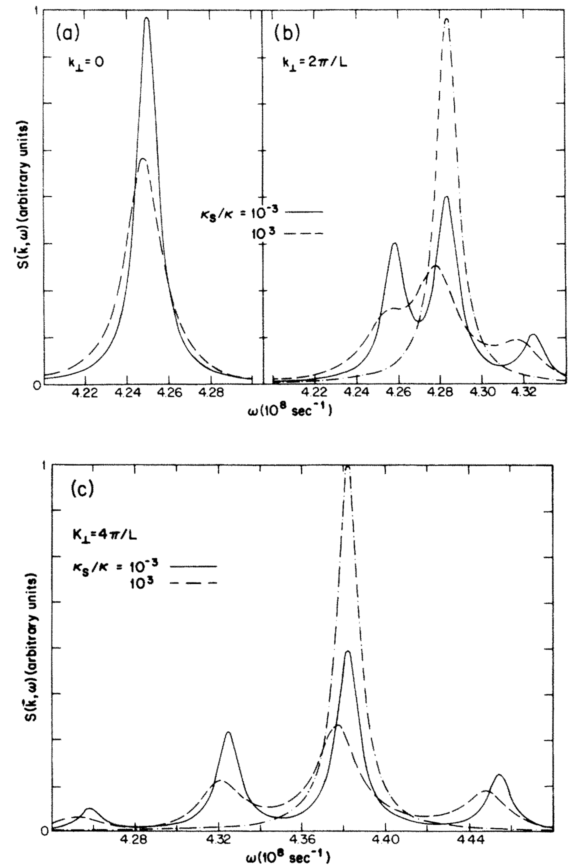

FIG. 5. Dynamic structure factor $S(\vec{k},\vec{k},\omega)$, for a fluid layer with slip boundary conditions, near the Brillouin frequency for $k_\perp=0$, $2\pi/L$, and $4\pi/L$, and $L=100$ μm. Other parameters are as in Fig. 1, but the solid curves pertain to poor thermal diffusivity of the solid ($\kappa_s/\kappa=10^{-3}$) while the dashed curves to high thermal diffusivity ($\kappa_s/\kappa=10^{3}$). Brillouin peak of the infinite fluid (dot-dashed curve) is shown for comparison.

VII. SUMMARY AND CONCLUSIONS

Using the linearized hydrodynamic theory of equilibrium fluctuations, we obtained exact expressions for the dynamic structure factor $S(\vec{k},\vec{k}',\omega)$ for a fluid layer confined by two parallel solid walls, in terms of the static structure factor $S(\vec{k},\vec{k}')$. We found that in such fluid layers, $S(\vec{k},\vec{k}',\omega)$ is a symmetric matrix in $k_\perp$ and $k'_\perp$ with nonvanishing off-diagonal elements, even if $S(\vec{k},\vec{k}')$ is assumed to be diagonal. The correlations between the Fourier modes with different values of $k_\perp$ arise because these modes do not satisfy the appropriate

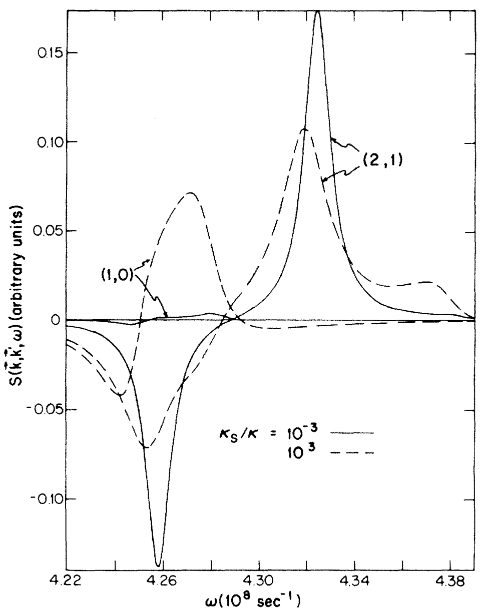

FIG. 6. Off-diagonal elements of the dynamic structure factor $S(\vec{k},\vec{k}',\omega)$, for a fluid layer with slip boundary conditions, near the Brillouin frequency for different values of $k_\perp = 2\pi n/L$ and $k'_\perp = 2\pi n'/L$ with $L = 100\ \mu$m. Curves are labeled (n,n'). Other parameters are as in Fig. 1, but the solid curves pertain to poor thermal diffusivity of the solid ($\kappa_s/\kappa = 10^{-3}$), while dashed curves pertain to high thermal diffusivity ($\kappa_s/\kappa = 10^3$). Scale is set by the Brillouin peak of the infinite fluid with $k_\perp = k'_\perp = 0$.

boundary conditions on the hydrodynamic variables; i.e., they cannot be the normal modes of the system. In the Fourier-series representation, this introduces modes coupling even in a linearized theory.

We find that the dynamic structure factor depends strongly on the energy and tangential momentum transport across the fluid-solid interfaces. In addition to a variety of waveguide modes which exist in such fluid layers, we also find new interfacial modes. These interfacial modes are essentially sound modes propagating parallel to the interfaces; there are two such modes for each distinct interface. These modes exist for nonvanishing transport of either energy or tangential momentum; i.e., they disappear for slip boundary conditions on the velocity field and for thermally insulating ($\kappa_s = 0$) rigid solid boundaries.

In general, the dispersion relation for the interfacial modes depends only on the component of the wave vector parallel to the boundaries $k_{\parallel}$ and the height L of the fluid layer. Their amplitudes, however, depend also on $k_\perp$ and $k'_\perp$. We found simple analytic expressions for the dispersion relation and amplitudes of these modes in extreme limits of tangential momentum transport (stick or slip boundary conditions) and for intermediate energy transport ($0 \le \kappa_s/\kappa \le \infty$) for sufficiently large values of L. In this case, the dispersion relation is independent of L, and for $\kappa_s = 0$ or ∞ with stick boundary conditions, or $\kappa_s = \infty$ with slip boundary conditions, the interfacial modes differ from the ordinary sound modes only in that their attenuation is enhanced. The additional dissipation may be due to the shear created by "sticky" solid boundaries and to the heat conduction between the fluid and solid when $\kappa_s \neq 0$ and the sound is not isothermal ($\gamma \neq 1$). The former effect introduces the dependence of the additional attenuation on shear viscosity ν, and the latter on thermal diffusivity of the fluid κ. In the intermediate cases of energy transport across the fluid-solid interface, the interfacial modes have a speed which is no longer the adiabatic sound speed but may have nonanalytic dependence on $k_{\parallel}$. For sufficiently large L, it has been shown that the amplitudes of the interfacial modes are inversely proportional to the layer height L. The criteria for the values of L, for which these modes provide a significant contribution to the dynamic structure factor, are also given. It turns out that for typical fluid parameters and wave vectors typical of light scattering experiments, the interfacial modes become important for $L \le 100\ \mu$m.

The dependence of the dynamic structure factor on the transport of energy and tangential momentum across the fluid-solid interfaces suggests that the experimental study of the dynamics of equilibrium fluctuations may provide a useful probe of interfacial transport over a wide frequency range in the hydrodynamic regime. Thus, interfacial transport can be studied by light scattering which measures directly the diagonal elements of the dynamic structure factor. Also, the measurements of sound propagation and attenuation in such fluid layers can be used to determine the dispersion relation for the interfacial modes and thus infer the underlying interfacial transport.

The experimental study of the dynamics of equilibrium fluid fluctuations would enable one to establish under what conditions the simple empirical models of interfacial transport, considered in this paper, are valid. Since the interfacial transport may depend on the interface preparation, it should be possible, for example, to study the effect of surface roughness on the tangential momentum transport across the fluid-solid interfaces, and thus to establish whether this roughness is the physical cause of stick boundary conditions on the velocity field. Other effects which may influence the dispersion relation and amplitudes of interfacial modes in fluid layers include, for example, acoustic excitations in solid boundaries and heterogeneous catalysis at the interfaces. The former effect will influence the normal momentum transport across such interfaces. The latter effect, because of the changes of enthalpy and, possibly, the number density of various fluid components at the interfaces due to catalytic reactions, may provide a new experimental tool for studying the kinetics of such reactions.

APPENDIX A

The matrix of eigenvectors of the matrix $\underline{M}$ is

$$\underline{A}=\begin{bmatrix} A_1 & A_1 & A_2 & A_2 & 0 & 0 \\ \lambda_1 A_1 & -\lambda_1 A_1 & \lambda_2 A_2 & -\lambda_2 A_2 & 0 & 0 \\ -\lambda_1 & \lambda_1 & -\lambda_2 & \lambda_2 & 1 & 1 \\ -\lambda_1^2 & -\lambda_1^2 & -\lambda_2^2 & -\lambda_2^2 & \lambda_3 & -\lambda_3 \\ k_{\|}^2 & k_{\|}^2 & k_{\|}^2 & k_{\|}^2 & -\lambda_3 & \lambda_3 \\ \lambda_1 k_{\|}^2 & -\lambda_1 k_{\|}^2 & \lambda_2 k_{\|}^2 & -\lambda_2 k_{\|}^2 & -\lambda_3^2 & -\lambda_3^2 \end{bmatrix}, \tag{A1}$$

and its inverse matrix is

$$\underline{A}^{-1}=b_0\begin{bmatrix} x_2\lambda_3 & -x_3\lambda_2 b_1 & \lambda_2\lambda_3^2 A_2 b_1 & -\lambda_3 A_2 & -\lambda_3 A_2 & \lambda_2 A_2 b_1 \\ x_2\lambda_3 & x_3\lambda_2 b_1 & -\lambda_2\lambda_3^2 A_2 b_1 & -\lambda_3 A_2 & -\lambda_3 A_2 & -\lambda_2 A_2 b_1 \\ -x_1\lambda_3 & x_3\lambda_1 b_1 & -\lambda_1\lambda_3^2 A_1 b_1 & \lambda_3 A_1 & \lambda_3 A_1 & -\lambda_1 A_1 b_1 \\ -x_1\lambda_3 & -x_3\lambda_1 b_1 & \lambda_1\lambda_3^2 A_1 b_1 & \lambda_3 A_1 & \lambda_3 A_1 & \lambda_1 A_1 b_1 \\ (x_2-x_1)k_{\|}^2 & 0 & \lambda_1\lambda_2(A_2-A_1)k_{\|}^2 b_1 & (A_1-A_2)k_{\|}^2 & (A_1\lambda_2^2-A_2\lambda_1^2) & \lambda_1\lambda_2(A_2-A_1)b_1 \\ (x_1-x_2)k_{\|}^2 & 0 & \lambda_1\lambda_2(A_2-A_1)k_{\|}^2 b_1 & (A_2-A_1)k_{\|}^2 & (A_2\lambda_1^2-A_1\lambda_2^2) & \lambda_1\lambda_2(A_2-A_1)b_1 \end{bmatrix} \tag{A2}$$

where

$$A_i \equiv -\frac{(\gamma-1)}{\alpha}\frac{x_i}{s+\gamma\kappa x_i}, \tag{A3}$$

$$b_0 \equiv \frac{1}{2\lambda_3(A_1x_2-A_2x_1)}, \tag{A4}$$

$$b_1 \equiv \frac{\gamma\kappa\lambda_3 x_1 x_2}{s\lambda_1\lambda_2 x_3} = -\frac{\lambda_3}{\lambda_1\lambda_2}\frac{\gamma\nu s}{c^2+s\gamma\Gamma_v}. \tag{A5}$$

APPENDIX B

Coefficients c_i in the case of stick boundary conditions are

$$c_1=-[U_2g_1+A_2(P_2+\delta_T)(g_2+P_3g_3)]/2T(U), \tag{B1}$$

$$c_2=-[V_2g_1+A_1(S_2+\delta_T)(g_2+S_3g_3)]/2T(V), \tag{B2}$$

$$c_3=[U_1g_1+A_1(P_1+\delta_T)(g_2+P_3g_3)]/2T(U), \tag{B3}$$

$$c_4=[V_1g_1+A_1(S_1+\delta_T)(g_2+S_3g_3)]/2T(V), \tag{B4}$$

$$c_5=\{k_{\|}^2(S_1-S_2)g_1+k_{\|}^2[A_1(S_1+\delta_T)-A_2(S_2+\delta_T)]g_2+[A_1S_2(S_1+\delta_T)-A_2S_1(S_2+\delta_T)]g_3\}/2T(V), \tag{B5}$$

$$c_6=\{k_{\|}^2(P_1-P_2)g_1+k_{\|}^2[A_1(P_1+\delta_T)-A_2(P_2+\delta_T)]g_2+[A_1P_2(P_1+\delta_T)-A_2P_1(P_2+\delta_T)]g_3\}/2T(U), \tag{B6}$$

where

$$T(U)\equiv A_1 U_2(P_1+\delta_T)-A_2 U_1(P_2+\delta_T)\ , \qquad \text{(B7)}$$

$$T(V)\equiv A_1 V_2(S_1+\delta_T)-A_2 V_1(P_2+\delta_T)\ , \qquad \text{(B8)}$$

$$U_i\equiv P_i-k_{\|}^2 P_3\ , \qquad \text{(B9)}$$

$$V_i\equiv S_i-k_{\|}^2 S_3\ . \qquad \text{(B10)}$$

APPENDIX C

Coefficients c_i in the case of slip boundary conditions are

$$c_1=-[g_1P_2+g_2A_2(P_2+\delta_T)]/2T(P)\ , \qquad \text{(C1)}$$

$$c_2=-[g_1S_2+g_2A_2(S_2+\delta_T)]/2T(S)\ , \qquad \text{(C2)}$$

$$c_3=[g_1P_1+g_2A_1(P_1+\delta_T)]/2T(P)\ , \qquad \text{(C3)}$$

$$c_4=[g_1S_1+g_2A_1(S_1+\delta_T)]/2T(S)\ , \qquad \text{(C4)}$$

$$c_5=0\ , \qquad \text{(C5)}$$

$$c_6=0\ , \qquad \text{(C6)}$$

where

$$T(P)\equiv A_1P_2(P_1+\delta_T)-A_2P_1(P_2+\delta_T)\ , \qquad \text{(C7)}$$

$$T(S)\equiv A_1S_2(S_1+\delta_T)-A_2S_1(S_2+\delta_T)\ . \qquad \text{(C8)}$$

[1]D. Gutkowicz-Krusin and I. Procaccia, Phys. Rev. Lett. 48, 417 (1982).
[2]H. Lamb, *Hydrodynamics* (Dover, New York, 1945).
[3]L. D. Landau and E. M. Lifshitz, *Fluid Mechanics* (Pergamon, Oxford, 1951).
[4]B. Berne and R. Pecora, *Dynamic Light Scattering* (Wiley, New York, 1976).
[5]S. Richardson, J. Fluid Mech. 59, 707 (1973).
[6]R. Zwanzig, J. Chem. Phys. 68, 4325 (1978).
[7]M. Redwood, *Mechanical Waveguides* (Pergamon, Oxford, 1960).